TIDE AND TIDAL CURRENT IN THE BALI STRAIT, INDONESIA

Dessy Berlianty[1,2,*] and Tetsuo Yanagi[2]

[1]Institute for Marine Research and Observation (BROK), Ministry for Marine Affairs and Fisheries, Jl. Baru Perancak, Br. Dangin Berawah, Ds. Perancak, Negara, Jembrana, BALI, 82251, Indonesia
[2]Research Institute for Applied Mechanics, Kyushu University, 6-1 Kasuga Koen, Kasuga, Fukuoka 816-8580, Japan
[*]Corresponding author and present address: Research Institute for Applied Mechanics, Kyushu University, 6-1 Kasuga Koen, Kasuga, Fukuoka 816-8580, Japan,
E-mail: dessyberlianty@yahoo.com

Received: 08 August 2011 Accepted: 02 October 2011

Abstract

Tide and tidal current model of the Bali Strait in Indonesia is produced by using a Coupled Hydrodynamical-Ecological Model for Regional and Shelf Seas (COHERENS). With its resolutions in the horizontal (500 meters) and the vertical (4 layers), the model well reproduces the four major tidal constituents, namely M_2, S_2, K_1, and O_1 tides, and their currents. Furthermore the model is used to investigate the tide-induced residual flow and tidal front in the Bali Strait. As a results, the tide-induced residual flow in the Bali Strait during the spring tide on May 16th in 2010 can be attributed to the variation of the strength of two eddies. The first one is the clockwise circulation in the shallow area at the wide part of the strait, while the second one is the small clockwise circulation in the south of the narrow strait. On the other hand, as suggestion from Simpson and Hunter (1974), the tidal front is determined by the value of $log(H/U^3)$ (where is the water depth in meters and the amplitude oftidal current amplitude in ms^{-1}). The front detected by the image of sea surface temperature distribution from the satellite corresponds with the contour $log(H/U^3)$ of 6.5.

Keywords: COHERENS**,** residual flow, tidal front, Bali Strait, SST image.

INTRODUCTION

The location of the Bali Strait in Indonesia is between Java Island and Bali Island (Fig. 1), and connecting the Java Sea and the Indian Ocean in the northern part and the southern part of the strait, respectively. Topography of the Bali Strait is shallow in the middle of the narrow strait, and steep at south of the strait, because it directly faces to the Indian Ocean.

Various studies in this strait have been conducted. Salijo (1973) and Burhanuddin and Praseno (1982) in Merta (1995), describes the presence of upwelling process in the Bali Strait, where the strait becomes so fertile that the biomass of the resource becomes very high. It makes this strait famous among fishermen in South Java and Bali, especially with Bali Sardinella (*Sardinella lemuru*), locally called lemuru. As more explanation by Merta (1995), amongst small pelagic fish exist in Indonesian waters, ikan lemuru which concentrates in the Bali Strait is one of the most important species. Researches by Hendiarti *et al.* (2005) and Susanto and Marra (2005) confirmed that the Bali Strait is an upwelling area, and it has rich nutrient with high biological and fisheries productivity.

In order to understand the physical phenomena to support primary productivity in the Bali Strait under the limitation to obtain enough qualified observed data, the numerical experiment could be the way to understand the structure of the physical and biochemical processes on a wide temporal and spatial scale (Yanagi, 1999). The previous studies of tidal characteristics has been carried out in larger-domain of Indonesian Seas, such as Wyrtki (1961), Hatayama *et al*. (1996), and Ray

DOI : 10.14203/mri.v36i2.39

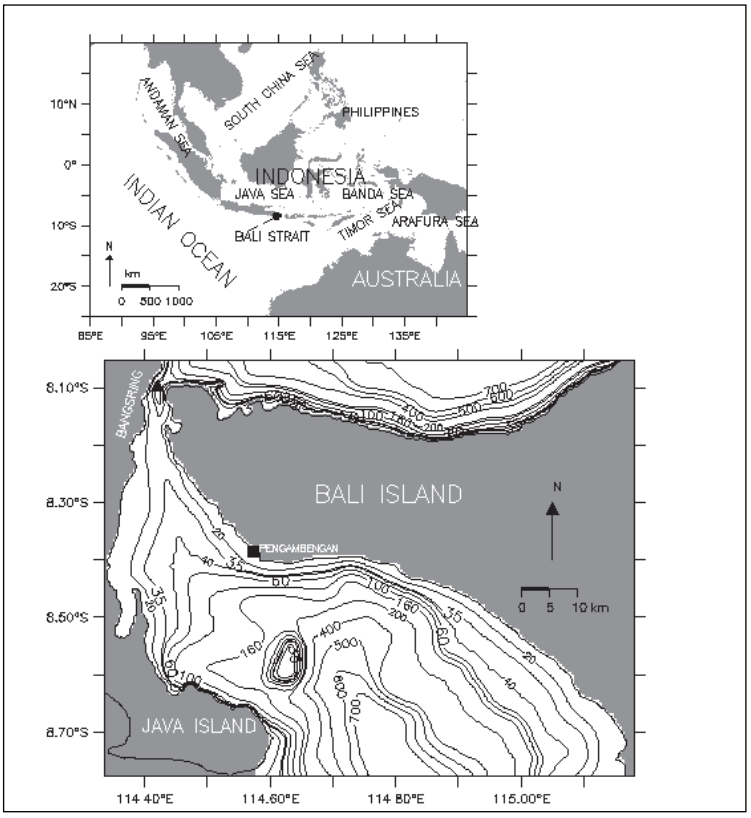

Figure 1. Indonesian Seawaters (upper) and bathymetric map of the Bali Strait, Indonesia (lower). Numbers show the depth in meters. Black cube shows the tide-gauge station and black triangle shows the current observation station.

et al. (2005). From the geographical distribution of the tidal types Wyrtki (1961) shows that the Bali Strait has mixed, prevailing semidiurnal tides is dominant, being an influence of the Indian Ocean. Hatayama *et al*. (1996) have investigated the characteristics of tides and tidal currents in the Indonesian Seas, with particular emphasis on the predominant constituents, the barotropic M_2 and K_1 components. Similarly, Ray *et al*. (2005) shows the cotidal charts of the largest semidiurnal tide M_2 and diurnal tide K_1 based on ten years of sea-level measurements from the Topex/Poseidon satellite altimeter. Even though their studies are presently used to identify the tidal characteristics of the Indonesian Seas with relatively spatial resolution, it has limitation, for example, being unable to identify such characteristics in the narrow straits, e.g. the Bali Strait. It motivates the objectives of this study by starting to investigate the hydrodynamic condition such the tide and tidal current in the Bali Strait by using A Coupled Hydrodynamical-Ecological Model for Regional and Shelf Seas (COHERENS). This objective is addressed with data collected at Bangsring for tidal current and Pengambengan for tide (Fig. 1).

Furthermore, this paper in particular also examines the study of tide-induced residual flow and tidal front according to Yanagi (1974). He pointed out that the tide-induced residual flow plays very important roles in the dispersion of matter in estuaries, as well as the explanation in his book (Yanagi, 1999) about tidal front which also plays a very important role in the primary production in the coastal sea. Mean while, to aim the examination of a tidal front, by using the detected front from the satellite image of sea surface temperature (SST), we seek the corresponding value of parameter $log(H/U^3)$, as suggestion from Simpson and Hunter (1974) that a tidal front is controlled and coincides by those critical parameter, where is the water depth in meters and the amplitude of the tidal current in ms^{-1}.

METHODS NUMERICAL MODEL

COHERENS Description

COHERENS is a three-dimensional multi-purpose numerical model for coastal and shelf seas (Luyten *et al.*, 1999). The COHERENS model is available for the scientific community and can be considered as a good tool for better understanding of the physical character of coastal sea and the prediction of waste material spreading there. Important advantages of the model are its transparency due to its modular structure and its flexibility because of the possibility of selecting different processes, specific schemes or different types of forcing for a particular application. This allows its use for process studies as well as for predictive or operational purposes without prior knowledge of its detailed structure. The hydrodynamic model is coupled to biological, resuspension and contaminant models, and resolves mesoscale to seasonal processes. The code has been developed initially over the period 1990 to 1999 by a multinational group as part of the Marine Science and Technology Programme (MAST) projects of Processes in Regions of Fresh Water Influence (PROFILE), North Sea Model Advection Dispersion Study (NOMADS), and COHERENS, funded by the European Union (Luyten *et al.*, 2002).

The governing hydrodynamic equations consist of the continuity equation and momentum equation. The Total Variation Diminishing (TVD) scheme is implemented in advection scheme for this model. The TVD scheme has the advantage of combining the monotonicity of the upwind scheme with the second order accuracy of the Lax-Wendroff scheme. Further details about the governing equations, numerical methods, and discretization schemes can be found in Luyten *et al.* (1999).

Numerical Scheme and Computational Grid

A study area of the Bali Strait is horizontally represented by a rectangular computational domain discretized with regular C-grid system. The horizontal grid is in the Cartesian coordinate system, the grid spacing is 500 m x 500 m, contained 180 x 160 grid points. Without considering temperature, ecology, thermo-dynamics and sediment, the model operates without the influences of the wind velocity and vertical stratification of temperature and salinity. Thus, the vertical water column is divided into 4 layers and the grid is vertically irregular as the result of –coordinate transformation.

Fig. 1 (lower) shows the topography of the Bali Strait, where the bathymetric data is obtained from Hydro - Oceanography Division – Indonesian Navy (DISHIDROS TNI AL), Bathymetric Map No. 290 with scale 1:200,000, edition of March 2006. The external time step of barotropic equations is to satisfy the Courant-Friedrichs-Lewy (CFL) criterion.

Calculation was run for 110 days from 11th February to 31st May, 2010 to cover the periods of tidal current and tide observations, on 18th to 19th February 2010 and 1st to 31st May 2010, respectively. In the interest of this study, to understand the physical phenomenon such tidal characteristics in the Bali Strait, have only utilizing the application of the physics model as one of the main program components of COHERENS (instead of biological model, sediment model, and contaminant model). There was no special treatment in order to attain convergence of the numerical solution since it was found by Luyten *et al.* (1999) that the model reaches good numerical convergence. On this study, the speciality output was made use of the program's utility of COHERENS to perform an harmonic analysis (by activated the *subroutine of defanal.f*), where the tide-induced residual flow, amplitude and phase are obtained by the program of harmonic analysis for the period of 15th– 17thof May 2010 (~ 6 tidal cycles) to examine its correspondence to the satellite data in the spring tide.

Initial and Boundary Conditions

The model on this study was initialized with zero elevation and velocity throughout the domain. Four main tidal components M_2, S_2, K_1, and O_1 were combined by using a global tide model ORITIDE (ORI.96; the Japanese high-resolution regional ocean tide model) to provide time series of surface elevations (Matsumoto *et al.*, 1995; 2000) along the open boundaries at northern and southern parts of the Bali strait (Fig. 1, lower).

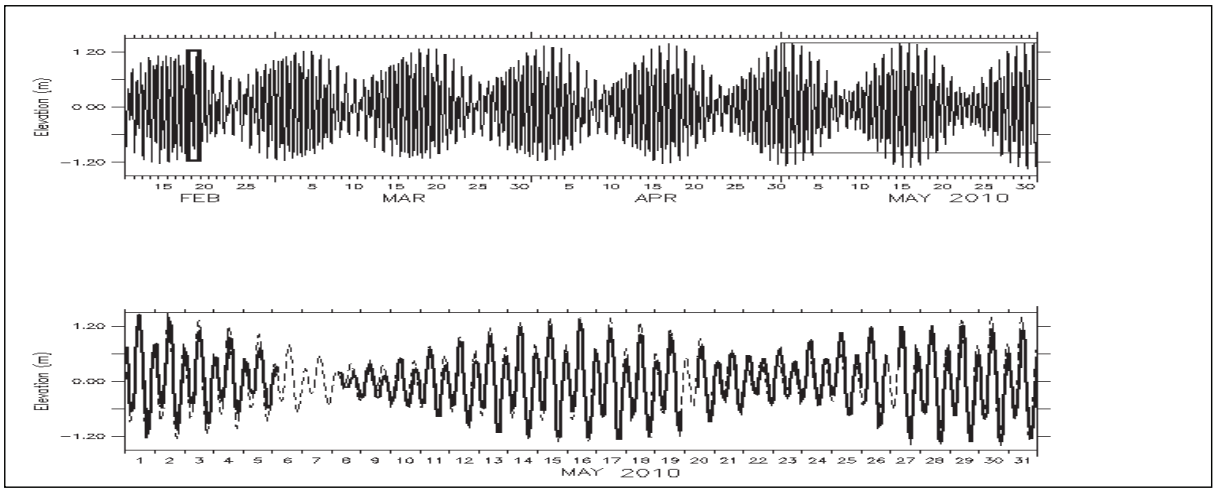

Figure 2. Simulation results (in meters) at Pengambengan Station for the period of February 11th to May 31th 2010. Thin box shows the period of elevation verification and bold box shows the period of current verification (upper). Verification of elevation (lower) between the observation data from Institute for Marine Research and Observation (full line) and the simulation results (dashed line) at Pengambengan for the period of May 1st to 31st 2010.

RESULTS AND DISCUSSION

Verification of elevation and current velocity

To test the capability of our 3-D model for tidal simulation, we ran the model forced directly by the global tidal elevation along the open boundary.

In this study, the elevation data by interval of 1 hours was obtained from the original tide-gauge time series at Pengambengan Station (marked with black cube on Fig. 1 (lower)), which belongs to the Institute for Marine Research and Observation, under the Ministry of Marine Affairs and Fisheries of Indonesia, whereas the current velocity data was observed at Bangsring Station (marked with black triangle on Fig. 1 (lower)). The current velocity observation depth was 20 meters and the data time interval was 20 minutes of vertically averaged profile records which was taken by using an Acoustic Doppler Current Profiler (ADCP) of SonTek Argonaut propeller.

Simulation results of elevation at Pengambengan Station for the period of February 11th to May 31st 2010 were shown in Fig. 2 (upper) where thin box shows the period of tidal verification and bold box showed the period of current verification.

Verification of elevation is shown in Fig. 2 (lower) to compare the observation data from Institute for Marine Research and Observation (full line) and the Simulation results (dashed line) at Pengambengan for the period of May 1st to 31st 2010. The simulated elevations were in good agreement with the observed data where the Root Mean Squared Error (RMSE) was 0.29 meters and the Root-squared (r^2) is 0.813.

Lower values of RMSE indicated the absolute fit of the model to the data points (how close the observed data to the model's predicted values), likewise values of r^2 close to the maximum range of one (value of 1) indicating that our model adequately fitted to the elevation data.

The calculated current velocities at Bangsring Station for the period of February 18th to 19th 2010 were shown in Fig. 3 and were compared to the observation of current velocity. The current velocity component of *U*; East-West direction and *V*; North-South direction indicated that simulation results were a little larger than the observation data (Fig. 3(a) and Fig. 3(b)).

Furthermore, Fig. 3c and d show that there is phase lag about three hours between the elevation and the current velocity at Bangsring Station (the narrow part of the strait). It could be simply explained in Yanagi (1999) by the vertically integrated equations of motion and continuity under the assumption of linear motion and non-viscous fluid in 1-dimension of the bay, as

$$\frac{\partial u}{\partial t} = -g\frac{\partial \eta}{\partial x} \text{ and } \frac{\partial \eta}{\partial t} + h\frac{\partial u}{\partial x} = 0$$

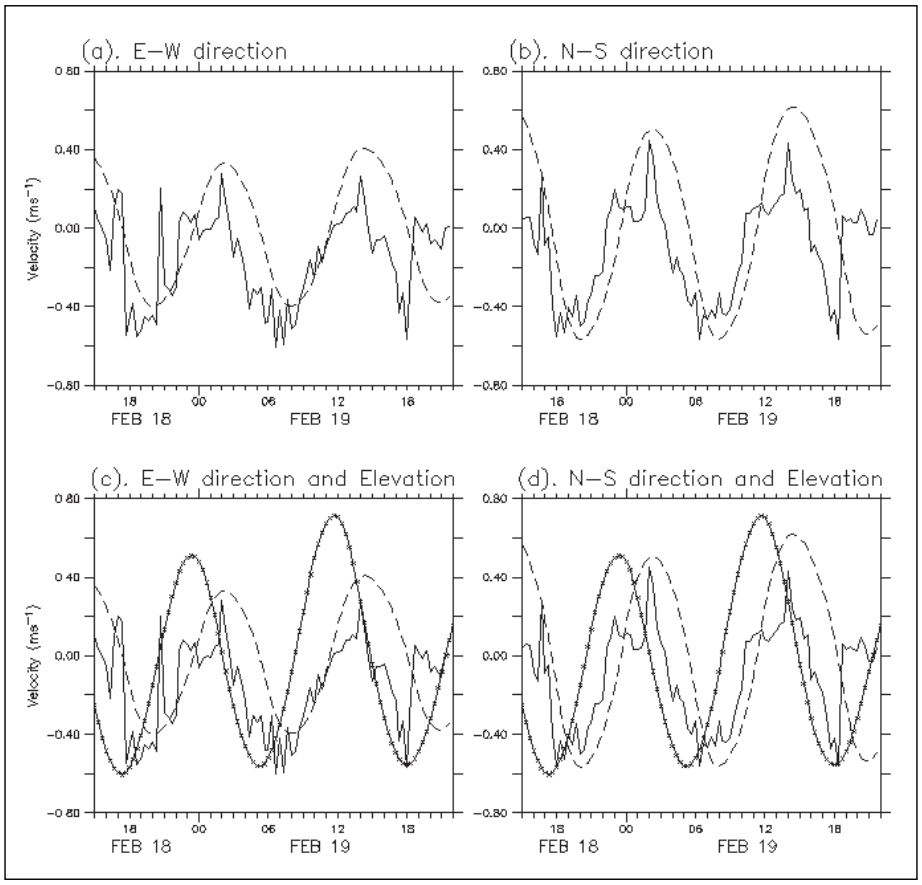

Figure 3. Verification of the current velocity component *U* in ms^{-1}; (*x*-direction, eastward (+) - westward (-)) in (a), and component *V* in ms^{-1}; (*y*-direction, northward (+) - southward (-) in (b), respectively, between the observation data at Bangsring Station (full line) and the simulation results (dashed line) for the period of February 18th to 19th 2010. Simulation results of elevation (in meters) at Bangsring Station for the period of February 18th to 19th 2010 (c and d) are compared to the current velocity component. Point-full line shows the elevation simulation, full line shows the current observation and dashed line shows the simulation results of tidal current.

with a uniform depth h and length l. Thus shortly, by assume that $u=U_0\sin(\sigma t)$ for x=l and u=0 for x=0, where $\sigma=2\pi/T$ and T denotes the tidal cycle and U_0 the tidal current amplitude, hereafter the solutions are easily obtained as,

$$\eta(x,t)=U_0\sqrt{\frac{h}{g}}\frac{\cos(kx)}{\sin(kl)}\cos(\sigma t) \quad \text{and}$$

$$u(x,t)=U_0\frac{\sin(kx)}{\sin(kl)}\sin(\sigma t)\,,$$

where k shows the wave number ($k=2\pi/L$), and L the wave length of the tidal wave.

Therefore, the solutions show that the phase of sea level variation and current variation differ by $\pi/2$(3 hours) and it indicates that the type of tidal wave in the narrow part of the Bali Strait is the standing wave, where the current direction goes north-eastward at ebb tide and south-westward at flood tide. Therefore, there is a little phase difference of tide and tidal current in the Bali Strait and the high water, low water, flood and ebb happen at nearly the same time.

Tide and Tidal Current

Figure 4a is the observed and calculated tidal amplitude spectrum at Pengambengan Station (in log scale and frequency spectrum). Both show a good agreement and the same peaks between observation data (full line) and simulation results (dashed line) appear. There are two group of peaks in Fig. 4a, where the first group indicates

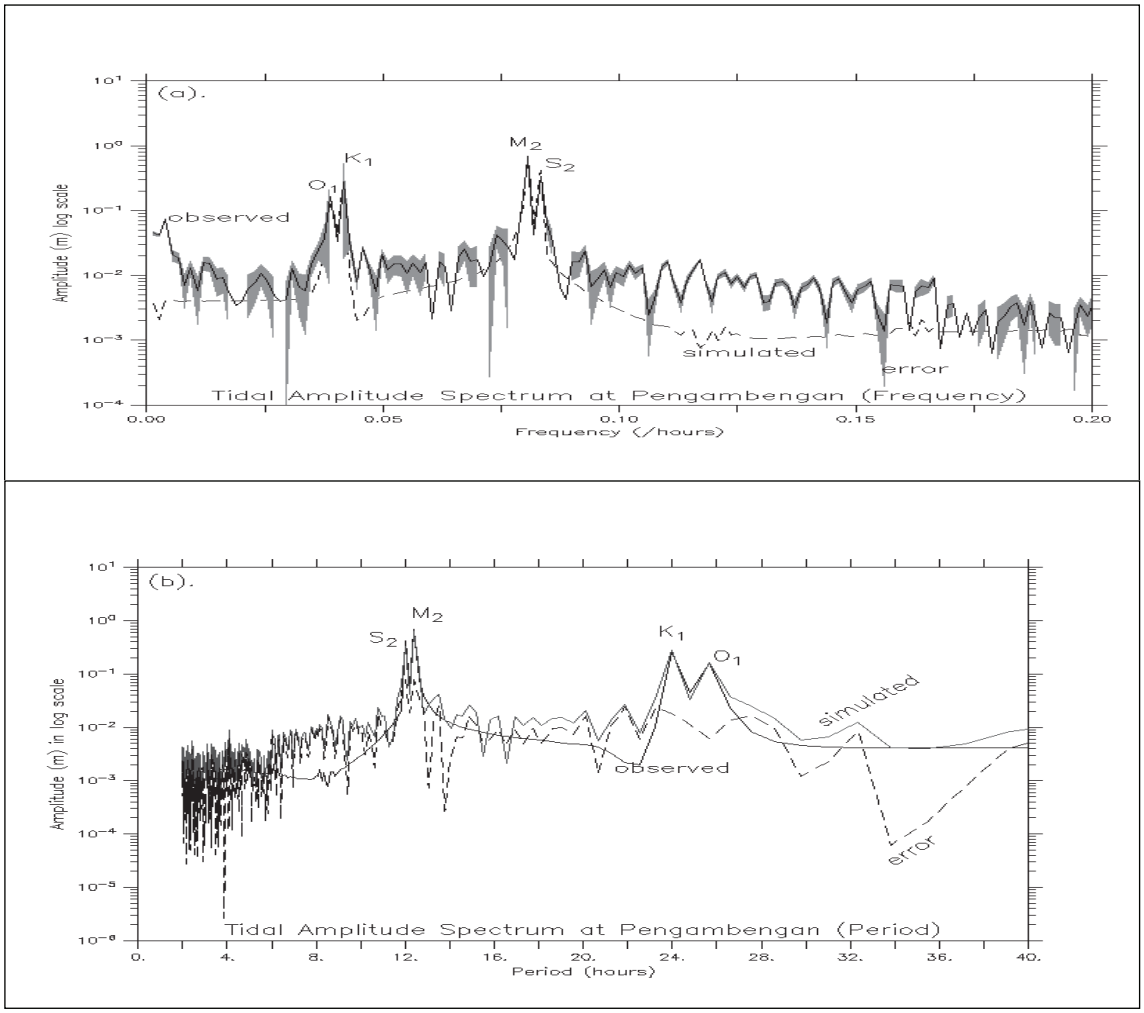

Figure 4. The tidal amplitude spectrum of the observed (full line) and simulated result (dashed line) at Pengambengan Station, with error swath in grey colour (upper graph), and similarly but in period axis (lower graph) for the tidal amplitude spectrum of the observed (thick line) and simulated result (thin line), with error in dashed line.

the semidiurnal period (Fig. 4(b), in log scale and period spectrum), i.e., around 12.4 hours (M_2) and 12 hours (S_2). Whereas, the second group indicates the diurnal period (Fig. 4b), i.e., around 23.9 hours (K_1) and 25.7 hours (O_1). The observed constituents amplitudes (thick lines of Fig. 4b) were used to calculate the tidal form factor (*F*) as defined by Pugh (1987), where the tidal factor

$$\frac{A_{K_1}+A_{O_1}}{A_{M_2}+A_{S_2}}$$

is 0.46 (represents the amplitude of the respective constituents, : A_{K_1}: 0.28 m, A_{O_1}: 0.16 m, A_{M_2}: 0.62 m, and A_{S_2}: 0.34 m). It denotes that the tide at Pengambengan Station can be classified into mixed, mainly semidiurnal ($0.25 < F < 1.5$) and it also confirms the tidal type of mixed tide prevailing semidiurnal at Bali Strait as mentioned in Wyrtki (1961).

Figure 5 and 6 show the simulated tidal current patterns in the Bali Strait during the spring tide (May 16th 2010) and the neap tide (May 22nd 2010), respectively. Tidal elevation at Pengambengan in Fig. 1 (lower) is chosen as the reference time of the flood and ebb conditions. The existence of currents with back and forth motion representing flood and ebb conditions is shown in Figs. 5 and 6.

The result of tidal current pattern at a maximum flood at high water in the spring tide shows that the currents flow into the strait through the

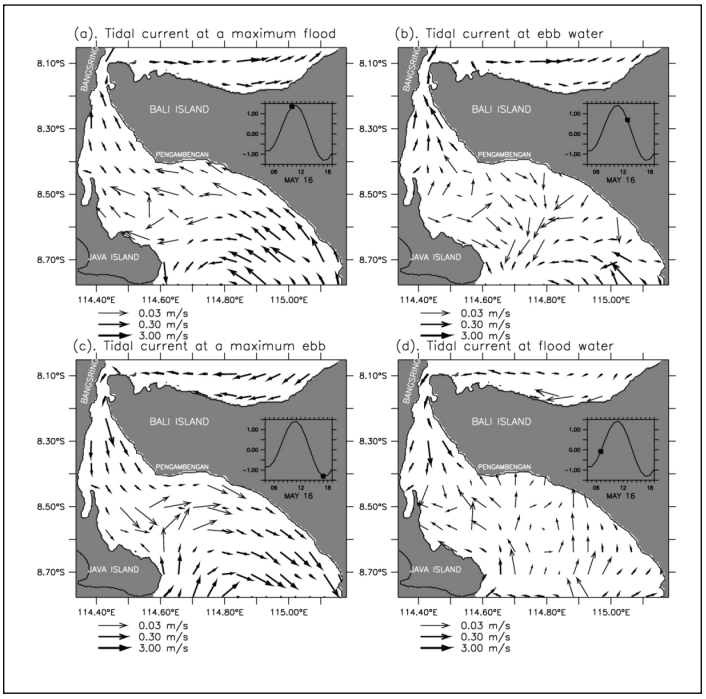

Figure 5. The calculated depth averaged tidal current at the spring tide of the Bali Strait (May 16th 2010), in ms^{-1} : (a) Tidal current at a maximum flood (high water), (b) Tidal current at ebb water, (c) Tidal current at a maximum ebb (low water), and (d) Tidal current at flood water.

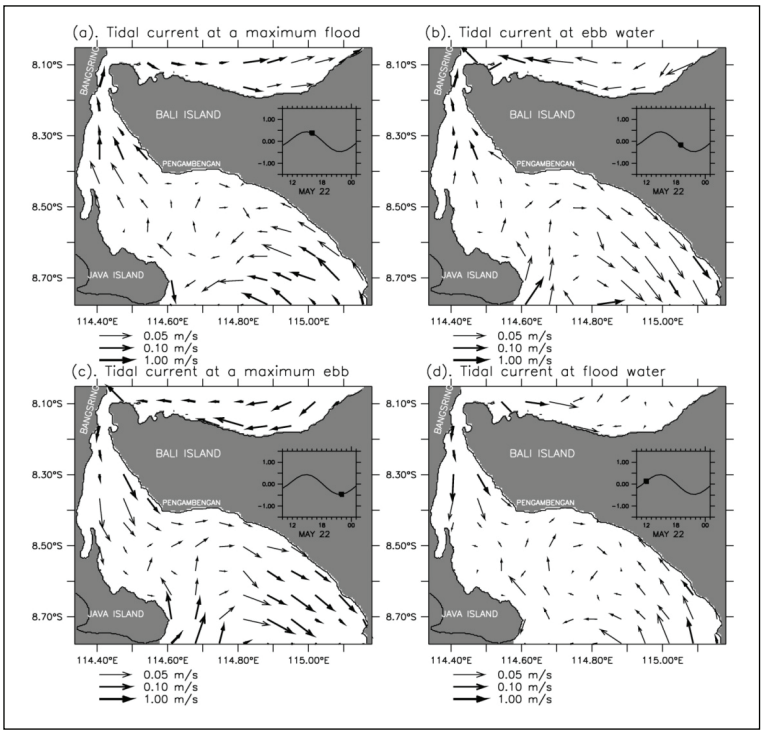

Figure 6. The calculated depth averaged tidal current at the neap tide of the Bali Strait (May, 22nd 2010), in ms^{-1}: (a) Tidal current at a maximum flood (high water), (b) Tidal current at ebb water, (c) Tidal current at a maximum ebb (low water), and (d) Tidal current at flood water.

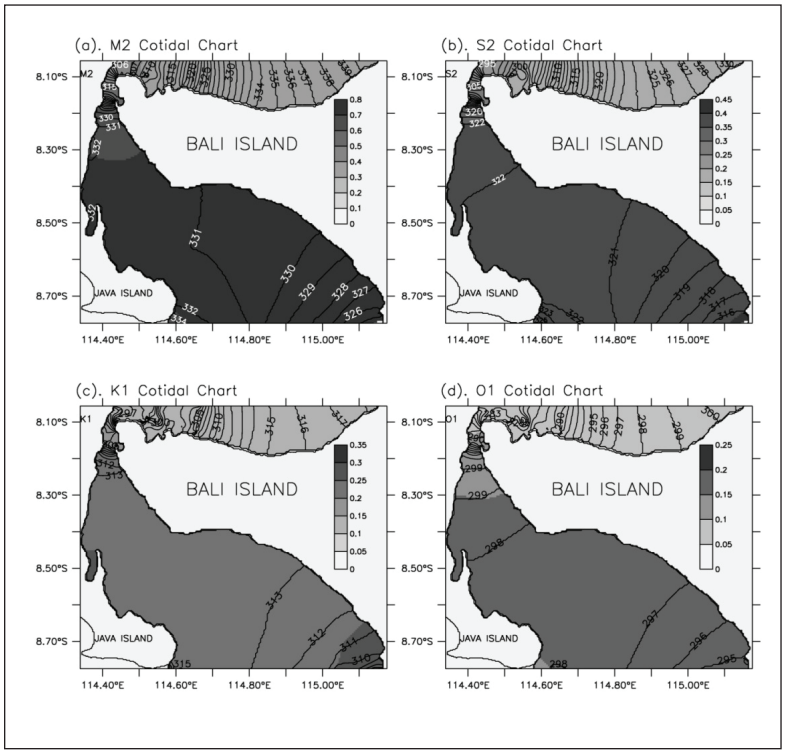

Figure 7. The calculated cotidal charts of four major constituents, grey filled contours denote the magnitude of the co-amplitude (in meters), and contour lines are the co-phase lines (°) referred to 8 h before GMT at 115°E

southern part of the strait with maximum velocity in the narrow strait of about 2 ms^{-1} (Fig. 5a). Tidal wave behaves as a progressive wave in the wide area of the Bali Strait. It could be explained as follows: if the tide is a progressive type in the open ocean, the maximum tidal current in the direction the wave is propagation coincides with the crest of the wave, or high tide (maximum flood). The maximum tidal current in the opposite direction coincides with the trough of the wave, or low tide (maximum ebb). During maximum ebb (Fig. 5c) at low water, the current keeps to flow to the south with velocity of about 0.5 ms^{-1} in the northern and southern parts The tidally-driven flow from the Indian Ocean into the wide strait perturb the mean flow in the Bali Strait and force a clockwise pattern of small tidally-generated eddy in the shallow area of the middle part of the wide strait at low water with the velocity of about 0.05 ms^{-1} (Fig. 5c).

The tidal current pattern at a maximum flood in the neap condition shows that the current is about 0.7 ms^{-1} in the narrow strait and the northern part of the strait (Fig. 6a). During maximum ebb, the current flows from the northern to southern parts of the strait at low water in the neap condition with maximum velocity of about 1.5 ms^{-1} and there is still an eddy in the shallow area of wide strait (Fig. 6c). There is an eddy in the shallow area of the wide part the Bali Strait during the neap tide (Fig. 6a - d).

Propagation of Tidal Waves

We have drawn the co-amplitude and co-phase charts of four major tidal constituents in the Bali Strait, i.e., M_2, S_2, K_1, and O_1 constituents in Figs. 7a - d, respectively, without those by field observation because there is no detailed-published chart for these four constituents.

As shown in the chart of Fig. 7a, M_2 tidal amplitude is about 0.71m in the south of the Bali Strait and decreases toward the middle area of the Bali Strait. As well shown, M_2 tidal amplitude becomes to minimum of 0.2 – 0.3m in the northern part of the strait.

Whereas, M_2 tidal phase of Fig. 7a shows the propagation of tidal wave mainly from the south-east of the Bali Strait to the narrow strait and to the

south-west of the Bali Strait (the Indian Ocean). It also shows that co-phases line in the north of the Bali Strait (the Java Sea) are distributed into two directions, tidal wave from the Java Sea firstly propagates to the narrow part of the Bali Strait and secondly propagates to the north coast of the Bali Island. Furthermore, in the narrow part of the Bali Strait, co-phase lines are gathered closely. Such feature suggests that the southward propagating tidal wave from the Java Sea comes across the northward propagating tidal wave from the Indian Ocean in the narrow part of the Bali Strait. This M_2 co-phase chart makes it clear that M_2 tidal waves in the Bali Strait are coming from the Java Sea and the Indian Ocean.

Almost the same as M_2 tide, S_2 tidal amplitude is about 0.4 *m* in the south of the Bali Strait and decreases from the south of the Bali Strait to the narrow area of the strait, as shown in Fig. 7b. S_2 co-phase line also shows the S_2 tidal wave propagation from the south and the north to the narrow part of the Bali Strait with almost the same characteristics as M_2 tide.

As shown in Fig. 7c, similarly to those of semidiurnal tides of M_2 and S_2, K_1 tidal amplitude decreases gradually from the south of the Bali Strait of 0.3*m* to the narrow area of the straits of 0.2*m*. K_1 co-phase lines show the same propagation characteristics as the semidiurnal tides of M_2 and S_2, from the Java Sea and the Indian Ocean.

O_1 tidal amplitude (Fig. 7d) also decreases gradually from the south of the Bali Strait of 0.2 *m* to the north area of 0.05 *m*, and almost the same in that area.

Residual Flow and Tidal Front

As described in Yanagi (1974), the residual flow plays an important role in the long-term dispersion of material in estuaries, and one of the main components of residual flow in the coastal sea is the tide-induced residual current. Tide-induced residual current is generated by the non-linearity of tidal current motion. Tidal current is essentially a divergence-convergence motion, i.e., the sea surface rises when the tidal current converges and falls when the tidal current diverges. On the other hand, the tide-induced

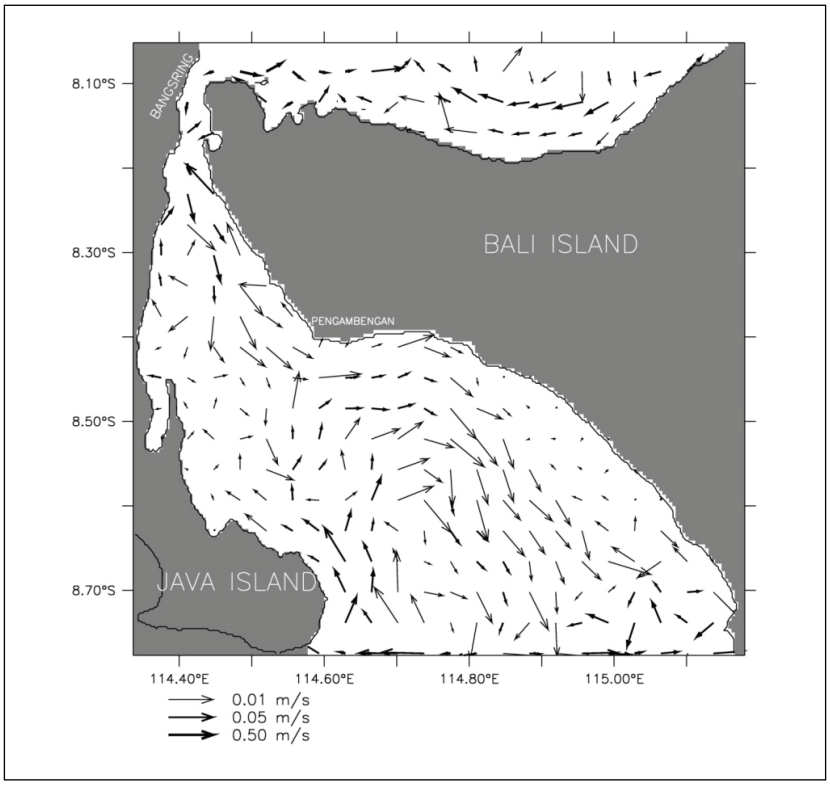

Figure 8. The calculated tide-induced residual current (depth averaged) of the Bali Strait during the spring tide on May 16th, in ms^{-1}.

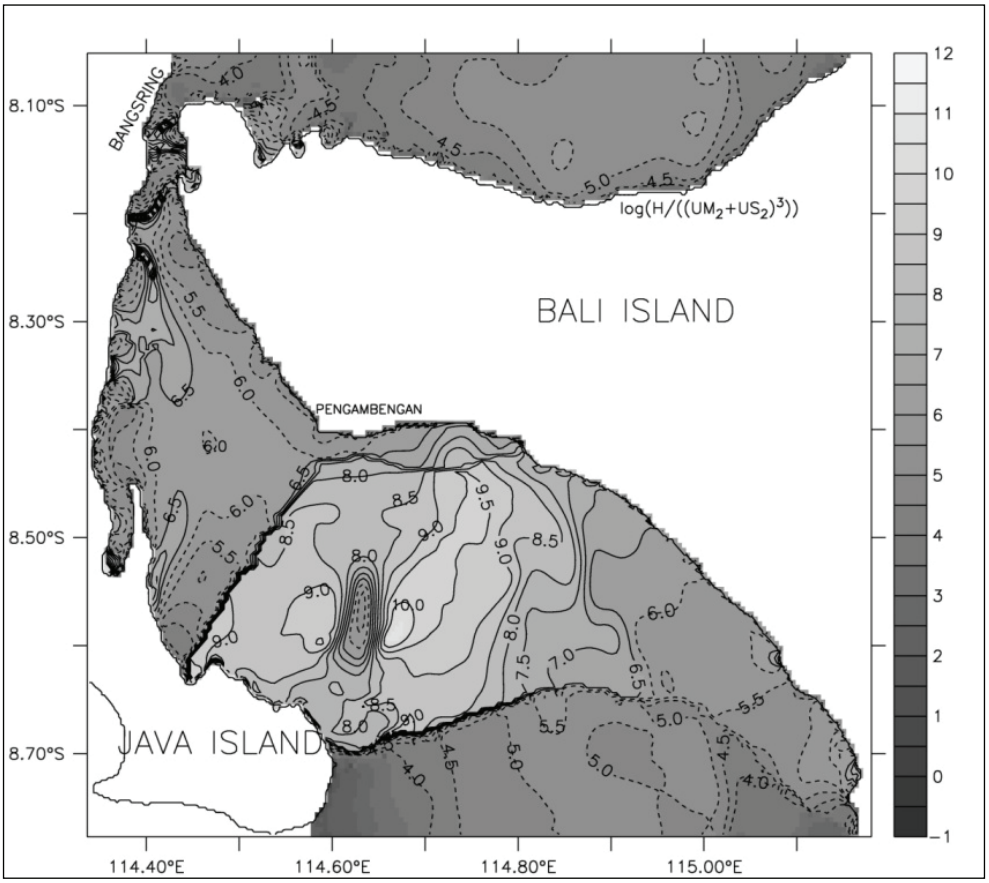

Figure 9. The calculated contour line of log(H/U^3) where H is the water depth in meters and U the amplitude of (M_2 + S_2) tidal current in ms^{-1}, dashed line show values less than 6.5, and full line show values great than 6.5.

residual current is essentially rotational motion: i.e. there is no divergence or convergence in the tide-induced residual current motion and it forms eddies (Yanagi, 1999).

Figure 8 shows the computed tide-induced residual current during the spring tide on May 16th in 2010 where there is a clockwise eddy with the speed of about 0.05 ms^{-1} in the shallow area at wide part of the Bali Strait and also a small clockwise eddy in the south of the narrow strait.

Otherwise, tidal front is a significant physical phenomenon in coastal waters. Tidal front plays an important role in the distribution of phytoplankton and zooplankton (Liu, *et al.*, 2003). One of important factors to generate the tidal front in the Bali Strait is considered to be the horizontal gradient of tidal current amplitude and water depth.

The calculated amplitude of four major tidal constituents shows that semidiurnal tides are more dominant than diurnal tides in the Bali Strait (Fig. 4). Therefore in order to investigate the position of tidal front, we examine $log(H/U^3)$ by using U of the amplitude of M_2+ S_2 tidal current in ms^{-1} and water depth. The results are shown in Fig. 9.

If we look satellite data (MODIS / Aqua 4 μm sea surface temperature images (nighttime) - Local Area Coverage (full-resolution data), Level-2 with time period: 8-day period beginning Monday, 17 May 2010 (nighttime), at 17:50 GMT on 20th May 2010 (Fig. 10), we can see the high water temperature occurred in the southern part of the Bali Strait. SST front exists in the central area of southern part of the Bali Strait, where the water depth change is large $log(H/U^3)$. value of 6.5 nearly coincides with the position of SST front (Figs. 9 and 10).

From the results in Figs. 9 and 10, when the sea-surface heating is dominant, a stratification develops in the central area of wide strait where the tidal current is weak, but the water is vertically well-mixed in the southern parts of the narrow

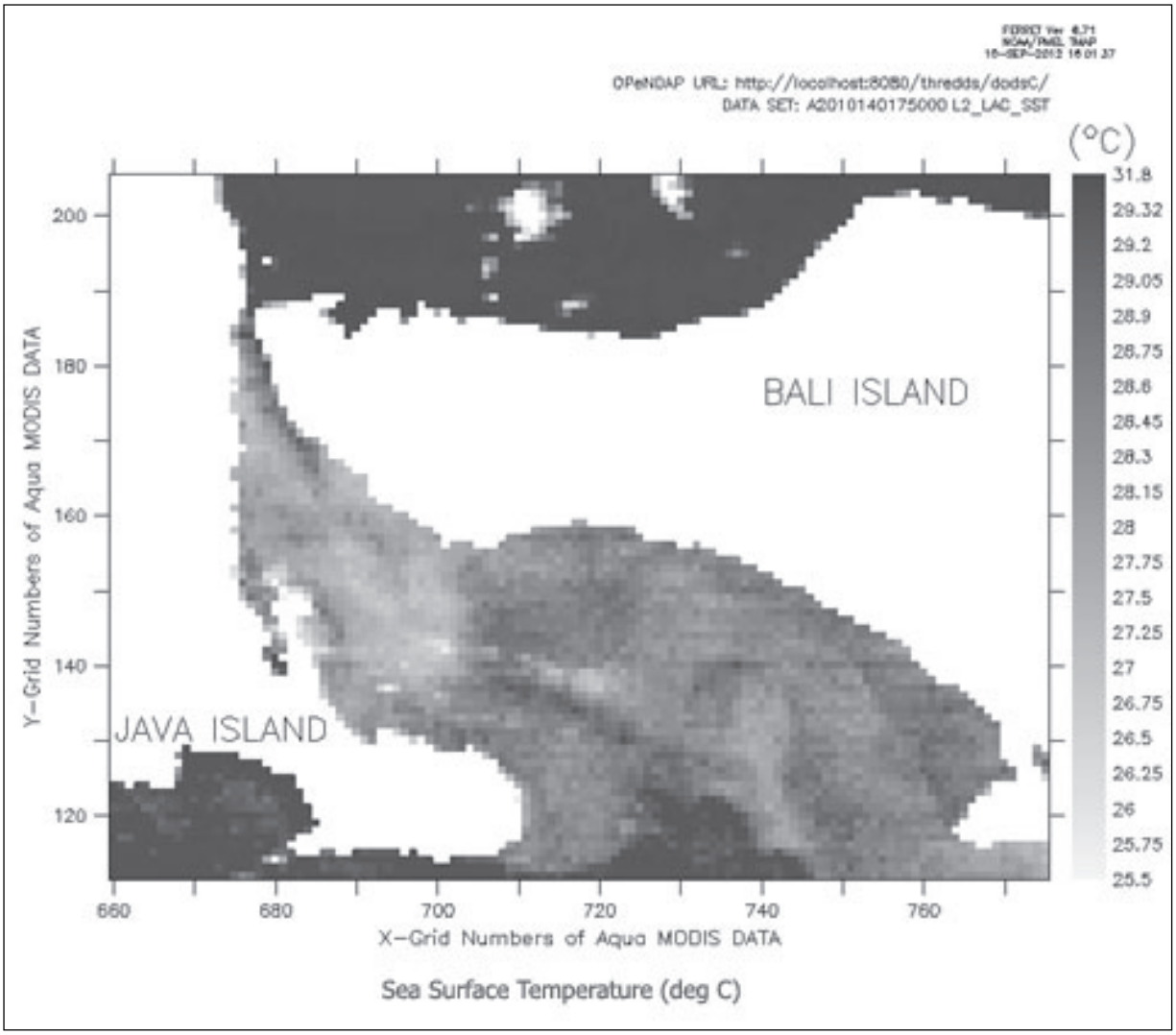

Figure 10. MODIS/Aqua 4 μm Sea Surface Temperature images (night time) - Local Area Coverage (full-resolution data), Level-2, with time period: 8-day period beginning Monday, 17 May 2010 (night time), at 17:50 GMT on 20th May 2010, showing the position of the tidal front in the Bali Strait. The dark areas on the satellite image indicate warmer water. The light area in the north of the strait is due to the colder water. North is at the top of the image and the grid size on the satellite image is 1 km^2.

strait and wide strait where the tidal current is strong. The tidal front is generated at the transition zone between the stratified and vertically well-mixed regions (Yanagi, 1999).

CONCLUSION

Using a high resolution three dimensional numerical model of COHERENS, the tides and tidal currents of M_2, S_2, K_1, and O_1 constituents in the Bali Strait are reproduced well. M_2 tide is most dominant and SST front is generated along the line of $log(H/U^3)$ of 6.5. The reason for producing such a distribution of tidal front and tide-induced residual flow in the model has been investigated.

Due to the limitations of the observed data, especially the observed tidal current data, some of the model results can be verified only in short period. On the other hand, it remains a problem to be solved in the future, to include the baroclinic tide and tidal current in the numerical model and to improve the precision of topography data.

Future work would consist of expanding model to be coupled with ecosystem model in order to simulate primary productivity distribution in the Bali Strait of Indonesia.

ACKNOWLEDGEMENTS

The author(s) wish to acknowledge use of the Ferret program for analysis and graphics in this paper. Ferret is product of NOAA's Pacific Marine Environmental Laboratory. Information is available at http://ferret.pmel.noaa.gov/Ferret/.

We would like to sincerely thank the Japanese Government Ministry of Science, Education and Sport (MEXT) who supports this work through a grant to the doctoral scholarship.

We also would like to thank Institute for Marine Research and Observation under Ministry of Marine Affairs and Fisheries of Indonesia for data support (the sea level data were collected time-series in the framework of the Operational Oceanography Project, funded by the Indonesian Government) and Prof. John Matthews for the short and fruitful discussions of MODIS data. We are also grateful to the anonymous reviewers for their valuable comments.

REFERENCES

Burhanuddin and D. Praseno, 1982. *Water Environment of the Bali Strait (in Indonesian)*. Proceeding of the "Lemuru" Fishery Seminar, (pp. 27−32). Banyuwangi.

Hatayama, T., T. Awaji and K. Akitomo. 1996. *Tidal* Currents in the Indonesian Seas and Their Effect on Transport and Mixing. *Journal of Geophysical Research* 101(C5): 12,353−12,373. 15 May 1996.

Hendiarti, N., Suwarso, E. Aldrian, K. Amri, R. Andiastuti, S. I. Sachoemar, I. B. Wahyono. 2005, Dec. Seasonal Variation of Pelagic Fish Catch Around Java. *Oceanography,* 18(4): 112−123.

Liu, G., S. Sun, H. Wang, Y. Zhang, B. Yang and P. Ji, 2003. Abundance of Calanus sinicus across the tidal front in the Yellow Sea, China. *Fisheries Oceanography*, 12 (4−5): 291−298.

Luyten, P., J. E. Jones, R. Proctor, A. Tabor, P. Tett and K. Wild-Allen. 1999. *COHERENS - A coupled hydrodynamical-ecological model for regional and shelf seas: User Documentation.* MUMM Report, Management Unit of the Mathematical Models of the North Sea, 914 pp.

Luyten, P., J. Jones and R. Proctor. 2002. A numerical study of the long and short term variability and thermal circulation in the North Sea. *Journal of Physical Oceanography*, 32: 37−56.

Matsumoto, K., M. Ooe, T. Sato and J. Segawa. 1995. Ocean tide model obtained from TOPEX/POSEIDON altimetry data. *Journal of Geophysical Research*, 100 (C12) 25: 319−25,330.

Matsumoto, K., T. Takanizawa and M. Ooe. 2000. Ocean tide model developed by assimilating TOPEX/POSEIDON altimeter data into hydrodynamical model: A global model and a regional model around Japan. *J. Oceanography*, 567−581.

Merta, I. G. 1995. A Review of Stock Assessment of Ikan Lemuru (*Sardinella lemuru*) in the Bali Strait. *IARD Journal*, 17(4): 71−76.

Pugh, D. T. 1987. *Tides, Surges, and Mean Sea Level.* John Wiley & Sons Ltd.

Ray, R. D., G. D. Egbert and S. Y. Erofeeva. 2005. The Indonesian Seas: A Brief Overview of Tides in the Indonesian Seas. *Oceanography*, 18(4): 74−79.

Salijo, B. 1973. *Oceanographic Condition of "Lemuru" Fish Catch Areas in the Bali Strait (in Indonesian)*. Lembaga Penelitian Perikanan Laut 2(42), 1−16.

Simpson, J. and J. Hunter, 1974. Fronts in the Irish Sea. *Nature*, 250, 404−406.

Susanto, R. D. and J. Marra. 2005. Effect of 1997/98 El Nino on Chlorophyll a Variability Along the Southern Coast of Java and Sumatra. *Oceanography*,18(4): 124−127.

Wyrtki, K. 1961. *Physical Oceanography of the Southeast Asian Waters.* La Jolla, California: The University of California-Scripps Institution of Oceanography.

Yanagi, T. 1974. Dispersion due to the residual flow in the hydraulic model. *Cont. Geophys. Inst.*, Kyoto Univ. 14: 1−10.

Yanagi, T. 1999. *Coastal Oceanography.* Tokyo: Terra Scientific Publishing Company.